Carbohydrate Polymers 98 (2013) 1565–1572

Contents lists available at ScienceDirect

Carbohydrate Polymers

journal homepage: www.elsevier.com/locate/carbpol

Nano-cellulosic materials: The impact of water on their dissolution in DMAc/LiCl

Merima Hasani[a,1], Ute Henniges[b,1], Alexander Idström[c], Lars Nordstierna[c], Gunnar Westman[a], Thomas Rosenau[b], Antje Potthast[b,*]

[a] Department of Chemical and Biological Engineering/Organic Chemistry, Chalmers University of Technology, SE-412 96 Gothenburg, Sweden
[b] Department of Chemistry/Division of Chemistry of Renewables, Christian-Doppler-Laboratory, Department of Chemistry, University of Natural Resources and Life Sciences, Konrad-Lorenz-Straße 24, A-3430 Tulln an der Donau, Austria
[c] Department of Chemical and Biological Engineering/Applied Surface Chemistry, Chalmers University of Technology, SE-412 96 Gothenburg, Sweden

ARTICLE INFO

Article history:
Received 25 March 2013
Received in revised form 8 June 2013
Accepted 3 July 2013
Available online 11 July 2013

Keywords:
Accessibility
Dissolution kinetics
Fibre morphology
Fibrillated cellulose
Gel permeation chromatography
Water content

ABSTRACT

The dissolution behaviour of disassociated cellulosic materials in *N*,*N*-dimethylacetamide/lithium chloride (DMAc/LiCl) was investigated. The parameters monitored were chromatographic elution profiles and recovered mass by means of gel permeation chromatography (GPC) with RI detection. In order to elucidate the impact of the disassembly on cellulosic fibres, comparative studies were performed with the non-disassociated cellulose counterparts. The importance of the presence of water was addressed by Karl Fischer titration and solvent exchange experiments. Morphological changes during the dissolution process were studied by scanning electron microscopy (SEM). Dissolution of fibrillated cellulosic materials is impeded compared to the non-fibrillated material. This is a consequence of the high-surface-area fibrils prone to retain high amounts of water. Dissolution behaviour of nano-crystalline cellulosic materials appeared to be source-dependent. Due to the absence of entangled networks, these materials retain only water bound at the surface of the nano-crystallites, indicative of both the exposed surface area and solubility. The small cellulose nano-particles extracted from dissolving pulp show lower solubility compared to the large NCC particles from cotton.

1. Introduction

As the prospect of utilizing nano- and micro-cellulosic materials as building blocks in new materials generates intense research activities, there is an increasing need for thorough characterization of these structures. Superior mechanical properties originating from the outstanding strength of cellulose crystals and pronounced hydrophilicity in combination with large surface area make them attractive components in composites, porous materials, and water retention applications.

On a molecular level, GPC-based methods including determination of molecular mass and monitoring of changes in molar mass distribution are important analytical tools. They rely on a complete, preferably direct dissolution of cellulose in non-degrading systems. Dissolution in the system DMAc/LiCl fulfils these requirements when performed under appropriate conditions (Dawsey & McCormick, 1990; McCormick, Callais, & Hutchinson, 1985; Potthast, Rosenau, Sixta, & Kosma, 2002). The general dissolution procedure of cellulose samples comprises a mechanical disintegration, followed by a solvent exchange from an aqueous system to DMAc and final dissolution in DMAc/LiCl (Ishii, Tatsumi, & Matsumoto, 2003).

However, dissolution of different types of cellulose in this system requires significantly varying conditions, as a function of fibre morphology, chemical composition and cellulose allomorphism (Henniges, Schiehser, Rosenau, & Potthast, 2010; Matsumoto, Tatsum, Tamai, & Takaki, 2001). Particularly challenging samples in this respect are pulps rich in lignin, softwood kraft pulps (Sjöholm, Gustafsson, Pettersson, & Colmsjö, 1997), and to some extent also pulps from annual plants (Dupont, 2003). Difficult dissolution of these materials is attributed to poor accessibility of cellulose chains and is reflected first of all in a significantly prolonged dissolution time (Dupont, 2003). In contrast, a complete dissolution of sulphite dissolving pulps requires only a few hours (Matsumoto et al., 2001). The course of dissolution of these cellulosics was recently studied by following changes in the molar mass distribution (MMD)

* Corresponding author at: Christian-Doppler-Laboratory, Department of Chemistry, University of Natural Resources and Life Sciences, Vienna, Konrad-Lorenz-Straße 24, A-3430 Tulln an der Donau, Austria. Tel.: +43 1 47654 6454; fax: +43 1 47654 6059.
E-mail addresses: merima.hasani@chalmers.se (M. Hasani), ute.henniges@boku.ac.at (U. Henniges), idstrom@chalmers.se (A. Idström), nordstierna@chalmer.se (L. Nordstierna), westman@chalmers.se (G. Westman), thomas.rosenau@boku.ac.at (T. Rosenau), antje.potthast@boku.ac.at (A. Potthast).
[1] These authors contributed equally.

0144-8617/$ – see front matter © 2013 Elsevier Ltd. All rights reserved.
http://dx.doi.org/10.1016/j.carbpol.2013.07.001

over time (Henniges, Kostic, Borgards, Rosenau, & Potthast, 2011). The dissolution process was interrupted at different time intervals, and the MMD of the dissolved fractions was determined. Significant differences in the dissolution behaviour between annual plant and wood cellulosic materials were observed. The latter displayed a fairly constant MMD shape throughout the whole process, whereas the MMD shape of the annual plants was subject to significant changes, indicating a favoured dissolution of low molar mass fractions in the initial stage of the dissolution.

According to our experience, disassociated cellulosic materials (nano-, micro- and fibrillated cellulosic materials) belong to yet another group of difficult-to-solve cellulose materials, which require long dissolution times and a special sample preparation procedure. Here, accessibility issues must be explained in different terms. During preparation of micro- and nano-cellulosic materials, the original cellulose substrates are disassociated into micro- and nano-elements of different nature: entangled networks of microfibrils in fibrillated cellulosic materials, and suspensions of highly crystalline nano-particles in nano-crystalline cellulosic materials. Probably the most prominent effect of these fragmentations is a dramatic increase in specific surface area. For instance, specific surface areas reported for paper and dissolving pulp grades, as measured by Congo Red adsorption, range between 1 and 20 $m^2 g^{-1}$, while those reported for micro-fibrillated and nano-crystalline cellulosic materials are in the ranges of 100–200 $m^2 g^{-1}$ and over 240 $m^2 g^{-1}$, respectively, i.e. one to two orders of magnitude higher (Goodrich, Bhattacharya, & Winter, 2009). As a direct consequence, the interaction with water is tremendously increased, leading to high water retention. This effect is even more pronounced in highly entangled networks of fibrillated cellulosic materials which show an extremely high resistance to dewatering. More than a tenfold increase in water retention value (WRV) has been reported for micro-fibrillated cellulose (MFC) prepared by mechanical fibrillation of paper grade pulps (Spence, Venditti, Rojas, Habibi, & Pavlak, 2010). However, this impact of the enlarged hydrophilic surface area is not limited only to the wet-state. Keeping in mind that the cellulosic surfaces almost always, even when principally dry ("oven dry"), are covered by so-called non-freezing water, the disassociated cellulosic materials will, under most conditions, exhibit a higher water content than their non-disassociated counterparts.

Usually preparation of disassociated cellulosic materials is to various extents also accompanied by cellulose chain scission, especially significant for isolation of NCC and fibrillation methods mediated by oxidative pre-treatments (Battista, Coppick, Howsmon, Morehead, & Sisson, 1956; Saito et al., 2009). Based on the previous studies on non-disassociated cellulosic materials from different origins this reduction of molar mass would be expected to facilitate the dissolution process. The contradictory poor solubility of disassociated cellulosic materials implies though that the molar mass parameter is of minor importance when it comes to these materials.

Furthermore, the conversion from pulps to nano- and micro-cellulosic materials often involves changes in crystallinity. This is especially evident for nano-crystalline cellulosic materials in which the objective of preparation is the removal of amorphous regions by controlled acidic hydrolysis. The resulting increase in crystallinity and in accessibility of cellulose nano-particles are other factors expected to influence the dissolution behaviour. In this study, the dissolution process of selected nano- and micro-structured cellulosic materials was analyzed by following changes in the MMD, weight-average molar mass (M_w), and recovered mass during the dissolution. A "solvent-peeling" approach comprising interruption of the dissolution process after different time intervals, as well as separation of the dissolved fractions and their GPC analysis, was used as the tool to monitor these changes.

Table 1
Cellulose substrates and their abbreviations.

Description	Abbreviation
Dissolving pulp from Eucalyptus	EDP
Nano-crystalline cellulose from EDP	NCCe
Cotton cellulose filter aid	WFP
Nano-crystalline cellulose from WFP	NCCw
Bleached softwood kraft pulp, fibre length 2.3 mm, used for mechanically prepared MFC	SWKP
Micro-fibrillated cellulose from SWKP	MFCs
Micro-fibrillated cellulose from SWKP with extended solvent exchange	MFCsx
Bleached softwood kraft pulp, fibre length 2.6 mm, used for TEMPO-oxidized nano-fibrillated cellulose	toSWKP
TEMPO-oxidized nano-fibrillated cellulose from toSWKP	toNFCs

In our effort to investigate the obtained GPC results in terms of changed water interactions, Karl Fischer titrations were used to analyze variations in water content of the studied materials immediately after the required solvent exchange in DMAc.

However, these titrations are aimed as a supporting tool in assessing the relationship between dissolution kinetics and water presence, not a technique providing us with exact info on water content of the samples.

Detailed analysis of the free and non-freezing water in this system would exceed the scope of this study and is left for the upcoming studies.

2. Experimental

2.1. Materials

N,*N*-dimethylacetamide (HPLC grade, Sigma–Aldrich or Promochem, Wesel, Germany) and lithium chloride (analytical grade, Sigma–Aldrich or VWR Prolabo, Leuven, Belgium) were used as received. Demineralized water was prepared by reverse osmosis. The Karl Fischer titration was performed with dry methanol for Karl Fischer titration, water content max. 0.01% and Hydranal composite 5 for Karl Fischer titration, 1 ml ~ 5 mg water (both supplied from Sigma–Aldrich). The chemicals were used as received and additionally protected by molecular sieves to minimize absorption of surrounding moisture.

2.2. Cellulosic substrates

Four different cellulosic substrates were studied and compared to disassociated materials obtained from them (Table 1). In order to emphasize the importance of the fragment size, two fibrillated and two nano-crystalline materials varying significantly in particle/fibril dimensions were prepared. The chosen substrates were:

- prehydrolysis kraft dissolving pulp from Eucalyptus – used for preparation of the small-particle-size nano-crystalline cellulose (EDP)
- cotton cellulose filter aid, no. 541 from Whatman – used here for preparation of the larger-particle-size nano-crystalline cellulose (WFP)
- bleached softwood kraft pulp of an average fibre length of 2.3 mm (SWKP) – used for purely mechanically prepared micro-fibrillated cellulose (MFC)
- bleached softwood kraft pulp of an average fibre length of 2.6 mm (toSWKP) – used for preparation of TEMPO-oxidized nano-fibrillated cellulose (toNFC), exhibiting an extremely large hydrophilic surface area due to an efficient fibrillation down to the thinnest cellulose fibrils.

Both types of softwood kraft pulp were produced from approximately 70% spruce and 30% pine. The bleaching sequence of the softwood kraft pulp is totally chlorine free (TCF) with the peroxide-based bleaching sequence: (OO)Q(OP)QT(PO). Their chemical composition is reported in the supporting information.

Nano-crystalline cellulosic materials (NCC) were obtained by sulphuric acid hydrolysis, as described elsewhere (Beck-Candanedo, Roman, & Gray, 2005; Hasani, Cranstone, Westman, & Gray, 2008). The type prepared from pulp consisted of smaller particles than the one prepared from cotton filter aid. (The AFM images are provided in the supplementary data.)

Micro-fibrillated cellulose was obtained from the Norwegian Paper Research Institute, PFI, prepared by extensive refining followed by the high-pressure homogenization (BlueTop BT 30.70H, 1-89.200 from SPX) at 1% concentration, 1000 bar, and three passes of softwood kraft pulp, average fibre length 2.3 mm.

TEMPO-oxidized nano-fibrillated cellulose was obtained by TEMPO-oxidation (Saito, Nishiyama, Putaux, Vignon, & Isogai, 2006) of the softwood kraft pulp of slightly longer average fibre length, 2.6 mm, followed by homogenization at 1% concentration, 200 bar, 1 pass.

2.3. Methods

2.3.1. Solvent peeling

For each material, ten sub-samples (each 20 mg, dry content) were prepared as follows: each sub sample was suspended in 200 ml of demineralised water and quickly (two times 10 s) disintegrated in a kitchen blender. Excess water was removed by suction filtration on Whatman filter aid no. 1 with 11 μm particle retention in liquid; each sample was briefly washed with ethanol, and then placed in a dry 4 ml glass vial with a tight screw cap.

NCC- and MFC-samples, existing as aqueous suspensions, were instead washed with ethanol by centrifugation for 15 min at 4500 rounds per minute followed by removal of the separated liquid.

The vials containing the ethanol-washed materials were left in 4 ml of DMAc overnight for solvent exchange. The excess DMAc was removed. The sample was now divided; each sub-sample was placed in a fresh 8 ml glass vial, and 2 ml of DMAc/LiCl 9% (v/w) was added. The vials were placed in a laboratory shaker regardless the different previous solvent exchange steps. After specific time intervals (5, 20, 40, 60, 90, 120, 240, 480, 1440, and 7200 min), the dissolution process was stopped by addition of pure DMAc; the final ratio of DMAc/LiCl 9% (w/v) and pure DMAc was 2:3 (v/v). Directly before GPC measurements, the dissolved fractions were filtered through a 0.45 μm PTFE filter.

2.3.2. Multiple solvent exchange of MFC-samples

For preparation of multiply solvent-exchanged samples, the amount of MFC corresponding to 20 mg of dry material was placed in a 4 ml glass vial with a screw cap and vigorously mixed with approximately 3 ml ethanol. The excess ethanol was removed by centrifugation, for 15 min at 4500 rounds per minute, and approximately 4 ml of DMAc was added to the sample. The sample was left in DMAc overnight for solvent exchange. Next day, the excess DMAc was removed by centrifugation, and approximately 4 ml of fresh DMAc was added. The procedure was repeated three times. After removing the fourth portion of DMAc, the sample was mixed with DMAc/LiCl (9% (w/v)) and subject to solvent-peeling analysis according to the procedure above.

2.3.3. GPC instrumentation

Gel permeation chromatography (GPC) measurements used the following components: online degasser, Dionex DG-2410; Kontron 420 pump, pulse damper; auto sampler, HP 1100; column oven, Gynkotek STH 585; multiple-angle laser light scattering (MALLS) detector, Wyatt Dawn DSP with argon ion laser ($\lambda_0 = 488$ nm); refractive index (RI) detector, Shodex RI-71. In order to avoid fluorescence originating from pulp components, half of the MALLS detectors are equipped with interference filters (488 ± 10 nm) that were used when appropriate. Data evaluation was performed with standard Astra, GRAMS/32, and Origin software. The following parameters were used in the GPC measurements: flow: 1.00 ml min^{-1}; columns: four PL gel mixedA LS, 20 μm, 7.5 mm × 300 mm; injection volume: 100 μl; run time: 45 min; *N*,*N*-dimethylacetamide/lithium chloride (0.9%, v/w), filtered through a 0.02 μm filter, was used as the mobile phase. The amount of dissolved material was determined from the RI signal using a dn/dc of 0.136 ml/g and a detector constant of $5.3200e^{-5}$ V^{-1}; both values were determined by the authors.

2.3.4. Determination of water content

The water content was determined on a V20 volumetric Karl Fischer titrator (Mettler Toledo). The sample mass introduced into the system varied, and was determined as precisely as possible before it was added to the system. The water content is calculated automatically by the titration device, based on the introduced mass of the respective sample. The determination stops automatically after achieving a pre-set minimum drift rate over time (25 μg min^{-1}). The result is given as percentage of water content in the sample.

Alternatively, some water content determinations were performed on a moisture analyzer MA35 (Sartorius) that is based on infrared heating of the sample. With this system, 1 g of sample was weighted to 1 mg precision on the integrated balance, and was heated to 105 °C until constant weight was achieved. The result is given as percentage of water content in the sample (average of three measurements).

2.3.5. Scanning electron microscopy

Samples for SEM analysis were prepared by interrupting dissolution at different time intervals by dilution with DMAc, extensive water wash and gold sputtering for 60 s. Instrumentation: Leo Ultra 55 FEG SEM at 1 kV accelerating voltage.

2.3.6. Solid-state ^{13}C NMR spectroscopy

All NMR experiments were performed on a Varian Inova-600 operating at 14.7 T, equipped with a 3.2 mm solid-state probe. Measurements were conducted at 298 K, with a MAS spinning rate of 15 kHz. The CP/MAS ^{13}C NMR spectra were recorded using a cross-polarization pulse sequence followed by proton decoupling during acquisition. Acquisition parameters included a 2.9 μs and 4.0 μs ^{1}H 90° and ^{13}C-pulse respectively, 1200 μs contact time, 25 ms acquisition time, 5 s recycle delay to allow for complete thermal equilibration, and 10,000 acquisitions for each spectrum. The data were processed by MestreNova 7.0.3 software. For all spectra, a Gaussian apodization of 30 Hz, phase correction, and a first-order polynomial baseline correction were used in the processing.

Two methods for measurements of the crystallinity index of cellulose samples with CP/MAS ^{13}C NMR were applied. The NMR resonance of the C-4 carbon in cellulose gives rise to two spectral signals at 87–93 and 80–87 ppm, from crystalline cellulose and from amorphous cellulose, respectively. By dividing the intensity of the signal at 87–93 ppm by the total area, the crystallinity index can be calculated (Newman, 1999). In addition, from spectral deconvolution of the two areas into four and three peaks respectively (Wickholm, Larsson, & Iversen, 1998), and sequential comparison of deconvoluted peaks originating from crystalline and amorphous parts, the corresponding crystallinity index can be calculated (Hult, Liitiä, Maunu, Hortling, & Iversen, 2002). In this study, both methods were used and the average value was reported.

To verify the quantitative comparison of the amorphous and crystalline intensities, an array of spectra, with different cross-polarization times of the two C-4 NMR areas, was recorded and compared. As the C-4 carbons are chemically equivalent regardless of their crystalline or amorphous structure, the only possible effect on their relative signal intensity, apart from relaxation recovery, is the contact time of the cross-polarization pulse (Larsson, Wickholm, & Iversen, 1997). As we found that the normalized signal intensity of crystalline cellulose is equal to that of the amorphous cellulose when using cross-polarization contact times below 2000 μs, a contact time of 1200 μs was chosen for all samples.

3. Results and discussion

3.1. Dissolution behaviour of crystalline cellulosic materials

In Figs. 1 and 2, the dissolution processes of the two nano-crystalline cellulosic materials – NCC from Whatman filter paper (WFP) and NCC from Eucalyptus dissolving pulp (EDP) – and their respective starting materials are compared to each other. Comparative solvent-peeling combined with GPC revealed considerably different developments of the MMD of nano-crystalline cellulosic materials compared to their starting materials and, at the same time, an interesting mutual resemblance of the two NCC types. The elution profiles of the starting materials show in accordance with the previously reported results, and typical of each of these cellulosics (Henniges et al., 2011) – a slow increase in dissolved material for WFP and an almost immediately constant profile, appearing already after very short dissolution times, for the EDP.

The acid hydrolysis of these substrates used to produce NCC leads in both cases to a clear decrease of the molecular mass, resulting in a delayed elution time, as evident from Fig. 1 and especially Fig. 2. However, NCCw exhibits a separated peak in the high molar mass area, indicative of material with low polydispersity and very high molar mass, which is not present in the starting material prior to hydrolysis. This peak may either comprise of aggregates which the solvent is not able to separate into individual molecules or, more likely, undissolved nanocellulosic crystals, which did pass the filter and the columns. The light scattering radius of about 70 nm and a very high M_w supports this view of very compact, i.e. crystalline structures. NCCe shows a shoulder in the low molar mass area, indicating the presence of highly degraded chains. The shoulders look different and elute at different times: in NCCe the shoulder is rather well separated and elutes at about 34 ml; the shoulder of NCCw is more closely associated to the bulk material. These features are indicative of differences in morphology, and hence accessibility, of the starting materials. In addition, elution profiles for NCCw are shifted to higher molar masses compared to those for NCCe, reflecting the higher level-off DP for hydrolysis of Whatman filter paper (Battista, 1950; Battista et al., 1956).

Furthermore, dissolution of NCCe is characterized by considerable fluctuations in elution profiles over time. At the initial dissolution stages, these profiles are dominated by relatively low molecular fractions and are, as expected, shifted towards higher molecular masses after longer time intervals (120 min). However, upon prolonged dissolution (1440 and 7200 min), the elution profile is shifted back to lower molecular masses – an initially unexpected behaviour, not previously observed for cellulose samples. These variations are, however, strongly indicative of heterogeneity of the NCC-materials and are to be explained by variations in structure, morphology, or size of cellulose nano-crystals. In addition, sulphate ester groups present on NCC sample surfaces may impede dissolution as well.

As nano-crystalline cellulosic materials consist of pure, highly crystalline nano-particles with the morphology defined by the elementary crystallites of cellulose, the composition, crystallinity and morphology can be excluded as sources of heterogeneity within the samples originating from the same starting material. Instead, since the preparation of NCC works through acid hydrolysis liberating nano-particles with a certain size distribution, the observed variations in MMD are to be associated with size variations and the extent of aggregation of cellulose nano-crystals. Variations in both the particle size and existence of aggregates are evident from the AFM images (see supporting information). When going towards smaller NCC-particles, the exposed surface area per total volume area will increase, resulting in higher water content, as the surface is always covered with at least a monolayer of water molecules. Since the presence of water is known to retard the dissolution process in DMAc/LiCl, the smaller particles – rich in water and consisting in average of shorter cellulose chains – will dissolve more slowly than the larger particles containing predominantly longer cellulose chains, but displaying a smaller specific surface area.

The comparison of the mass recovery values for the dissolved dissolving pulp and the NCC prepared from it shows, as expected, a dramatic difference between these two materials (Fig. 3). While the total mass recovery for the dissolving pulp was around 250 μg, the corresponding amount for the resulting NCC was less than 20 μg, reflecting the extremely slow dissolution process of the NCC as opposed to that of its starting material. The two possible explanations for this include differences in the surface area and morphological changes. Conversion of pulp to NCC is associated with a drastic increase of the surface area, leading to a significantly higher surface bound water content and hence severely impeded dissolution. In addition, the preparation of NCC comprises a significant removal of the amorphous regions of the starting material, and increased crystallinity plays a superior role in these samples. Increased crystallinity is, for instance, expected to retard the dissolution process further, whereas morphological changes might have varied impacts, depending on the characteristics of the starting material.

The importance of these factors is reflected in Fig. 3 (right), showing the mass recovery values for the Whatman filter paper and the derived NCC. In spite of the inevitable increase of surface area and crystallinity during the conversion of the filter paper to NCC, the NCC particles show higher mass recovery than the starting material, most likely because of the inaccessible morphology of the starting material.

The drastically lower solubility observed for NCCe as compared to NCCw emphasises even further the significance of the size of the isolated structural entities. It is well known that cellulose nanocrystals from pulp are significantly smaller than those isolated from cotton under same conditions (Habibi, Lucia, & Rojas, 2010). Consequently, NCCe displays a larger surface area with a higher content of the surface bound water retarding the dissolution.

3.2. Fibrillated cellulosic materials

The features of dissolution were even more pronouncedly changed upon fibrillation. A drastic difference in dissolution behaviour between the fibrillated pulps and their starting materials was evident from the concentration versus volume plots (Figs. 4 and 5), reflecting the very poor solubility of MFC and the almost complete insolubility of toNFC.

As the conversion of the studied pulps to fibrillated materials involves primarily morphological changes achieved during fibrillation, these changes are to be held responsible for the observed changes in solubility. Of course, in the case of TEMPO-derived NFCs, the issue of changed surface chemistry due to oxidation has to be considered as well. As the preparation of this material is optimized to generate individual micro-fibrils with maximum carboxylate content on the surface, the dissolution impediment due to a possible aldehyde-mediated crosslinking can be neglected.

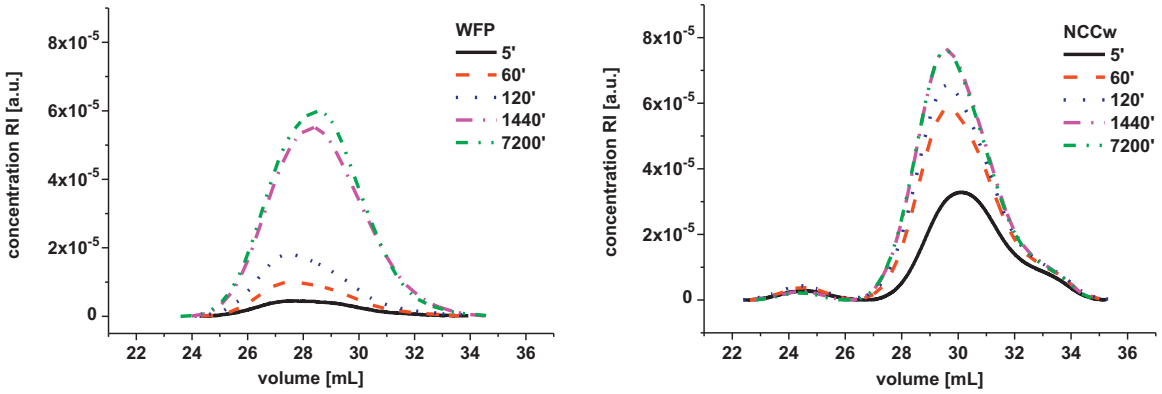

Fig. 1. Dissolution profiles by solvent-peeling in combination with GPC: volume versus concentration graphs of WFP (left) and NCCw prepared from WFP (right) at different dissolution times.

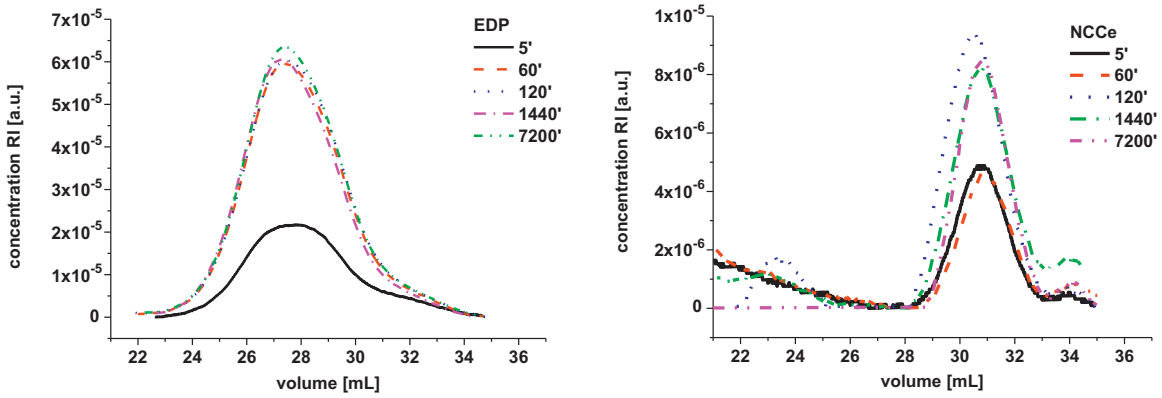

Fig. 2. Dissolution profiles by solvent-peeling in combination with GPC: volume versus concentration graphs of Eucalyptus dissolving pulp (EDP; left) and NCC prepared from EDP (right) at different dissolution times. Note the different scales of the concentration signal, indicating different amounts of dissolved material in EDP and NCCe.

The presence of carboxyls and the fact that fibrillation goes down to the thinnest individual fibrils are, on the other hand, very likely to interfere with the dissolution, as these factors significantly facilitate water retention.

The most prominent effect of fragmentation into smaller morphological entities upon fibrillation is an enhanced aspect ratio and a tremendous increase of the surface area. As discussed above, this implies increased water content originating from the surface-bound water layers, which, in turn, implies impeded dissolution. In an extreme case, such as the complete isolation of the thinnest individual fibrils during preparation of the toNFC, the generated surface is so large that the dissolution process is completely inhibited. Furthermore, a large surface area of cellulosic substrates is usually associated with an increased tendency to gel formation in swelling agents, a phenomenon that is likely to interfere seriously with the dissolution procedure in DMAc/LiCl. The occurrence of gelling in water and DMAc will hamper the removal of water by DMAc – an activation step necessary for a successful dissolution in DMAc/LiCl.

Comparing the development of the MMD profiles in Figs. 4 and 5 emphasises even further the drastic differences in the dissolution course of fibrillated and non-fibrillated pulps. In the case of MFC, only SWKP was used as raw material and therefore very comparable amounts and composition of hemicelluloses can be assumed. This was evident from the fact that the dissolution of the non-fibrillated

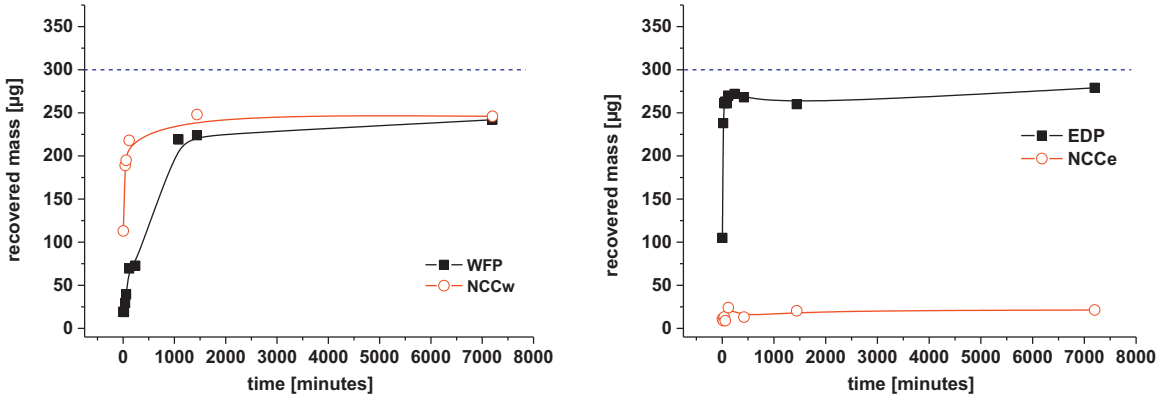

Fig. 3. Calculated mass recovery upon GPC analysis of WFP (left) and EDP (right) and the nano-crystalline cellulosic materials prepared there from. The dashed line corresponds to the theoretical maximum mass recovered, based on a 20 mg sample dissolved in 2 ml of DMAc/LiCl 9% after dilution filtration and injection, assuming no loss of sample.

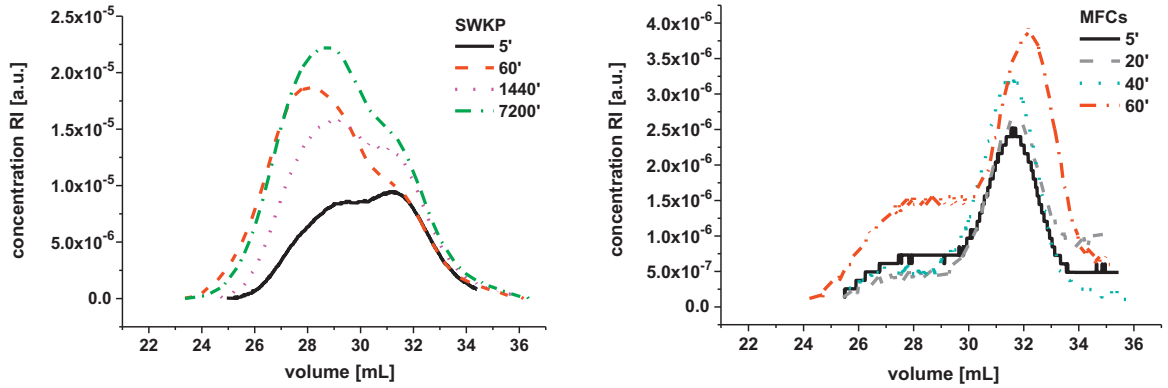

Fig. 4. Dissolution profiles by solvent-peeling in combination with GPC: concentration versus volume plots in the course of increasing dissolution time for starting pulp SWKP (left) and micro-fibrillated cellulose MFCs produced from it (right).

pulps follows the previously observed patterns, showing at early stages signals from predominantly low molecular fractions (hemicelluloses) that gradually transform into profiles dominated by long cellulose chains.

However, this relation between the dissolution time and the molecular mass of the dissolved fractions is no longer maintained by the fibrillated materials. For instance, the dissolution itinerary of MFC is instead reminiscent of that observed for NCCe, showing a MMD shift to lower molar masses after prolonged dissolution times. Again, this phenomenon reflects the heterogeneity of the micro-fibrillated cellulose stemming from the fibrillation process. Due to the strong inter-fibrillar forces, the separation of individual micro-fibrils is a very demanding and usually incomplete process. This is especially pronounced for pure mechanical fibrillation, relying on shear forces of varying local intensity. As a result, a range of micro-fibrils, fibrillar fragments and fibril bundles with a rather broad size distribution is generated (see the SEM analysis in Section 3.4). The smaller size fractions are generated by severe local forces involving considerable scission of cellulose chains. In larger bundles, having experienced milder conditions, this process occurs only to a minor extent, leaving predominantly long cellulose chains. In line with the previous discussion, these large bundles will be the first to dissolve (as they exhibit a smaller surface area), giving rise to the long-chain-dominated MMDs (at five and 20 min). On the other hand, dissolution of the smaller fractions will be impeded by their large surface area and will at longer time intervals give rise to MMD profiles dominated by shorter chains.

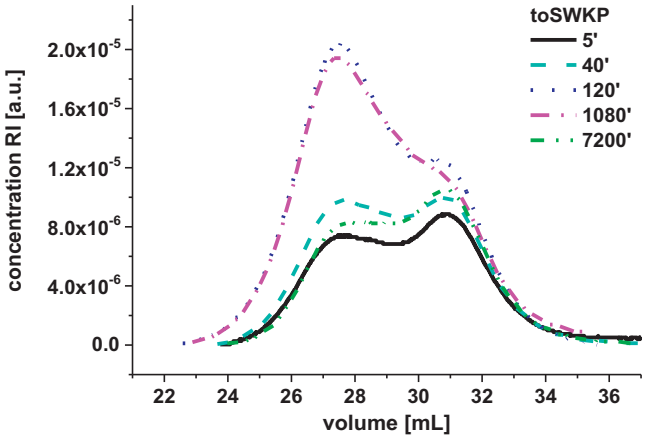

Fig. 5. Dissolution profiles by solvent-peeling in combination with GPC: concentration versus volume plots in the course of increasing dissolution time of toSWKP. No processable signal was obtained for the TEMPO-oxidized NFC prepared from it.

Interestingly, comparison of the elution volumes for MFC (Fig. 4) and NCC fractions (Figs. 1 and 2) shows a considerably lower concentration signal of the dissolved MFC fractions than of both NCC types. This in turn indicates a significantly lower solubility of MFC as a consequence of the water retaining entangled network.

3.3. Influence of the water content on dissolution behaviour

3.3.1. Fibrillated cellulosic materials

In order to study further the above discussed impacts of the surface area and the presence of water on the course of dissolution, the water content of the disassociated cellulosic materials and their starting materials was determined. Since the sample composition after the DMAc-activation is decisive for the subsequent dissolution in the DMAc/LiCl, the water content of the DMAc-activated samples (according to the standard solvent exchange procedure) was determined by Karl Fischer titration.

According to the titration results (Fig. 6), the fibrillated cellulosic materials show significantly higher water content after DMAc-activation compared to their starting materials, reflecting more porous fibrillated networks prone to binding and retaining relatively high amounts of water. A single solvent exchange with DMAc obviously fails to dehydrate these networks sufficiently,

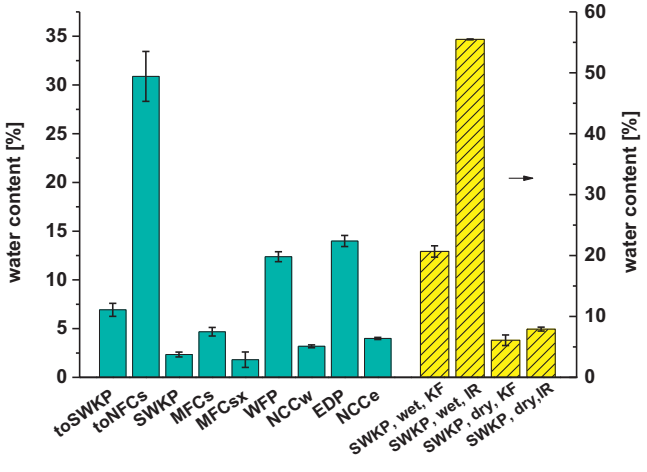

Fig. 6. Water content of disassociated cellulosic materials and their starting materials after activation with DMAc and prior to addition of DMAc/LiCl as determined by Karl Fischer titration (blue bars) and direct comparison of water content determination between IR moisture analyser and Karl Fischer titration (yellow striped bars). The titration method significantly underestimates the water content in the starting material SWKP. (For interpretation of the references to color in this artwork, the reader is referred to the web version of the article.)

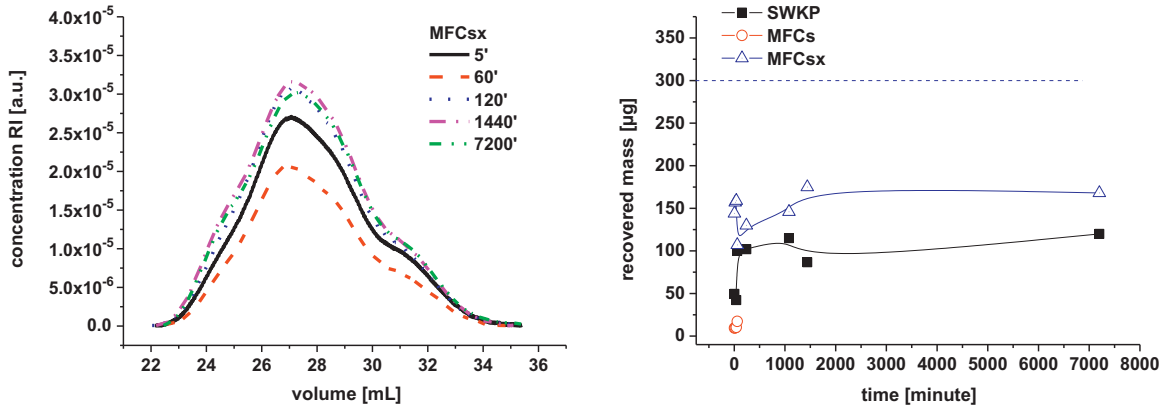

Fig. 7. Left: Dissolution profile at different dissolution times for MFC after multiple solvent-exchange treatment. For comparison, the corresponding plot for samples prepared with a single solvent exchange is shown in Fig. 4 right. Right: Calculated mass recovery of SWKP and the MFC prepared from it with and without multiple solvent-exchange treatment. The dashed line corresponds to the theoretical maximum mass recovered, based on a 20 mg sample dissolved in 2 ml of DMAc/LiCl 9% after dilution filtration and injection, assuming no loss of sample.

leaving them with too high a water content to allow unhindered dissolution in DMAc/LiCl. This is especially drastic in the case of toNFC, which retains over four times more water compared to its starting pulp. This behaviour originates from the liberation of the thinnest nano-fibrils with a highly hydrophilic surface, and is the reason behind the extremely poor solubility of this material in the DMAc/LiCl eluant. On the other hand, upon a repeated solvent exchange with DMAc, the water content of MFCs is appreciably reduced.

Subjecting the repeatedly solvent-exchanged MFC samples to the usual solvent-peeling analysis by GPC, a radically changed dissolution behaviour was revealed (Fig. 7). In contrast to the previously studied samples subjected to a single solvent exchange, the repeatedly solvent-exchanged MFC shows an extremely even dissolution with identical MMD profiles throughout the whole process. Moreover, the rate of dissolution is radically increased, even exceeding that of the starting pulp.

These results make it clear that water which can only be removed by repeated solvent exchange in DMAc is responsible for slow and uneven dissolution of MFC. After sufficient water removal, the differences between small and large fragments, i.e. between large and small surface areas containing water, are levelled out, and MFC starts to behave as a homogeneous material with regard to dissolution in DMAc/LiCl.

Interestingly, applying the repeated solvent-exchange procedure to toNFC did not improve solubility of this material, emphasizing once again the level of fibrillation, the binding ability of carboxyl groups towards water, and the morphology of the obtained material as decisive factors.

3.3.2. Nano-crystalline cellulosic materials

In contrast to fibrillated cellulosic materials, the DMAc-exchanged NCC samples showed significantly lower water content than their non-disassociated counterparts (Fig. 6).

However, this is rather an indication of the limitations of the titration method than the real picture of the condition of the samples. Complementary studies that determined water content by infrared drying to 105 °C were performed to compare the Karl Fischer titration to a standardized method (Fig. 6). The comparative studies of pulp samples with varying surface area and water content suggest that Karl Fischer titration indeed successfully measures water held by the fibrillar network, but fails to detect the surface-bound water, as this requires interruption of hydrogen bonds. Interaction between the Karl Fischer reagent and the surface-bound water molecules is obviously too weak to detach these molecules from the cellulose surface and make them accessible for the Karl Fischer reaction. As a consequence, the amount of water contained by DMAc-exchanged cellulosic materials is generally underestimated when measured by the volumetric Karl Fischer titration, as it reflects only the water loosely bound by the fibrillar network.

This underestimation is expected to be especially drastic in the case of NCC, as water held by DMAc-exchanged NCC-samples consists mainly of the surface-bound water. As a consequence, the Karl Fischer results do not correlate to solubility in DMAc/LiCl in this case.

3.4. Microscopy studies

The above reasoning on the dissolution of disassociated cellulosic materials was further supported by qualitative microscopy studies. The materials remaining after interrupted dissolution at different time intervals were analyzed by SEM. In the supporting materials sections the evaluation of SEM pictures emphasize the resistance of the disassociated cellulose to dissolution, as a consequence of its large (water-covered) surface area.

The images of dissolving pulp show obvious signs of dissolution after only 5 min, and complete dissolution after 60 min. Conversely, the images of MFC reflect only minor changes, while those of NCCe show hardly any changes during the first hour of dissolution.

Especially illustrative are the images of MFC confirming both the heterogeneity of the starting material and the course of dissolution outlined above. After only 5 min, the large MFC-fragments show signs of dissolution, observed as high molecular mass-MMD at the early dissolution stage. After 60 min, these large fragments are dissolved, leaving the rather homogeneous network of thin fibrils still essentially intact. The thinnest fibrils will be the last to dissolve, giving rise to relatively low recovered mass and causing the MMDs to be dominated by low molecular masses after long dissolution times.

4. Conclusion

The dissolution behaviour of disassociated (micro- or nano-structured) cellulosic materials in DMAc/LiCl is principally determined by the morphology and the exposed surface area generated upon fragmentation, and is thus strongly affected by the type of disintegration process and in some cases by the choice of starting material. This fragmentation is associated with severely impeded dissolution due to the liberation of a huge water-covered surface area. Generation of entangled networks additionally prone to retaining water can be an additional obstacle.

For instance, highly porous networks of fibrillated cellulosic materials contain a high percentage of surface-bound water held both within the fibrillar network and at the large fibril surface by hydrogen bonds. A single solvent exchange with DMAc employed in conventional dissolution procedures is not sufficient to remove this water in these cases. As a result, fibrillated cellulosic materials show extremely poor solubility when subjected to the common dissolution procedure in DMAc/LiCl. Instead, a repeated solvent exchange is required as efficient dewatering procedure in order to achieve satisfactory dissolution kinetics. As shown for micro-fibrillated cellulose, dewatering through repeated solvent exchange both increased the dissolution rate and erased heterogeneities originating from variations in surface areas (and thus hydration) of the MFC fragments.

However, this dewatering treatment proved not to be feasible with materials hindering solvent exchange by strong gelling in water, such as toNFC. The almost complete insolubility of this material, together with its pronounced resistance to solvent-exchange, emphasize even further the importance of the changed surface chemistry (carboxyl groups) and the degree of fibrillation correlating directly to the degree of entanglement and exposed surface – its chemistry, area and hydrophilicity.

The impact of the surface-bound water (and thus the surface area) of the material is particularly underlined by our studies of the two nano-crystalline cellulosic materials. Due to the absence of entangled networks under solvent exchange conditions, these materials essentially retain only water bound at the surface of the NCC-particles, indicative of both the exposed surface area and solubility. Accordingly, the small cellulose nano-particles extracted from dissolving pulp show significantly lower solubility compared to the large NCC particles from cotton.

With the improved understanding that this study provides of the forces that hinder cellulose dissolution in DMAc/LiCl and how to overcome them, future molecular analysis of nano- and micro-structured cellulosic materials by GPC are expected to become more reliable, facilitating quality control of production procedures for micro- and nano-structured cellulosic materials and their further processing.

Authors' contributions

The manuscript was written through contributions of all authors. All authors have given approval to the final version of the manuscript.

Acknowledgements

We thank Michael Obersriebnig (Department of Material Sciences and Process Engineering, University of Natural Resources and Life Science, Vienna) for performing atomic force microscopy on the samples, Sonja Schiehser (Department of Chemistry, University of Natural Resources and Life Science, Vienna) for assistance with GPC measurements and Alexander Bauer (Department of Sustainable Agricultural Systems, University of Natural Resources and Life Science) for providing access to the Karl Fischer titrator. Solid-state NMR measurements were conducted at the Swedish NMR Centre. The Södra Research Foundation and Gunnar Sundblads Forsknings-fond as well as the Austrian Christian Doppler Research Society (through the CD lab "Advanced cellulose chemistry and analytics") are especially acknowledged for financing the project.

Appendix A. Supplementary data

Supplementary data associated with this article can be found, in the online version, at http://dx.doi.org/10.1016/j.carbpol.2013.07.001.

References

Battista, O. A. (1950). Hydrolysis and crystallization of cellulose. *Industrial and Engineering Chemistry*, *42*, 502–507.

Battista, O. A., Coppick, S., Howsmon, J. A., Morehead, F. F., & Sisson, W. A. (1956). Level-off degree of polymerization: Relation to polyphase structure of cellulose fibers. *Industrial and Engineering Chemistry*, *48*, 333–335.

Beck-Candanedo, S., Roman, M., & Gray, D. G. (2005). Effect of reaction conditions on the properties and behavior of wood cellulose nanocrystal suspensions. *Biomacromolecules*, *6*, 1048–1054.

Dawsey, T. R., & McCormick, C. L. (1990). The lithium chloride/dimethylacetamide solvent for cellulose: A literature review. *Journal of Macromolecular Science, Part C: Polymer Reviews*, *30*, 405–440.

Dupont, A-L. (2003). Cellulose in lithium chloride/*N*,*N*-dimethylacetamide, optimisation of a dissolution method using paper substrates and stability of the solutions. *Polymer*, *44*, 4117–4126.

Goodrich, J. D., Bhattacharya, D., & Winter, W. T. (2009). Cellulose and chitin as nanoscopic biomaterials. In L. A. Lucia, & O. J. Royas (Eds.), *The nanoscience and technology of renewable biomaterials* (pp. 207–229). Chichester, UK: John Wiley & Sons. Ltd.

Habibi, Y., Lucia, L. A., & Rojas, O. J. (2010). Cellulose nanocrystals: Chemistry, self-assembly, and applications. *Chemical Reviews*, *110*, 3479–3500.

Hasani, M., Cranstone, E. D., Westman, G., & Gray, D. G. (2008). Cationic surface functionalization of cellulose nanocrystals. *Soft Matter*, *4*, 2238–2244.

Henniges, U., Kostic, M., Borgards, A., Rosenau, T., & Potthast, A. (2011). Dissolution behavior of different celluloses. *Biomacromolecules*, *12*, 871–879.

Henniges, U., Schiehser, S., Rosenau, T., & Potthast, A. (2010). Cellulose solubility: Dissolution and analysis of problematic cellulose pulps in the solvent system DMAc/LiCl. In T. F. Liebert, T. J. Heinze, & K. J. Edgar (Eds.), *Cellulose solvents: For analysis, shaping, and chemical modification. ACS symposium series* (Vol. 1033) (pp. 165–177).

Hult, E-L., Liitiä, T., Maunu, S. L., Hortling, B., & Iversen, T. (2002). A CP/MAS ^{13}C-NMR study of cellulose structure on the surface of refined kraft pulp fibers. *Carbohydrate Polymers*, *49*, 231–234.

Ishii, D., Tatsumi, D., & Matsumoto, T. (2003). Effect of solvent exchange on the solid structure and dissolution behavior of cellulose. *Biomacromolecules*, *4*, 1238–1243.

Larsson, P. T., Wickholm, K., & Iversen, T. (1997). A CP/MAS ^{13}C NMR investigation of molecular ordering in celluloses. *Carbohydrate Research*, *302*, 19–25.

Matsumoto, T., Tatsum, D., Tamai, N., & Takaki, T. (2001). Solution properties of celluloses from different biological origins in LiCl/DMAc. *Cellulose*, *8*, 275–282.

McCormick, C. L., Callais, P. A., & Hutchinson, B. H. R. (1985). Solution studies of cellulose in lithium chloride and *N*,*N*-dimethylacetamide. *Macromolecules*, *18*, 2394–2401.

Newman, R. H. (1999). Estimation of the lateral dimensions of cellulose crystallites using ^{13}C NMR signal strengths. *Solid State Nuclear Magnetic Resonance*, *15*, 21–29.

Potthast, A., Rosenau, T., Sixta, H., & Kosma, P. (2002). Degradation of cellulosic materials by heating in DMAc/LiCl. *Tetrahedron Letters*, *43*, 7757–7759.

Saito, T., Hirota, M., Tamura, N., Kimura, S., Fukuzumi, S., Heux, L., et al. (2009). Individualization of nano-sized plant cellulose fibrils by direct surface carboxylation using TEMPO catalyst under neutral conditions. *Biomacromolecules*, *10*, 1992–1996.

Saito, T., Nishiyama, Y., Putaux, J-L., Vignon, M., & Isogai, A. (2006). Homogeneous suspensions of individualized microfibrils from TEMPO-catalyzed oxidation of native cellulose. *Biomacromolecules*, *7*, 1687–1691.

Sjöholm, E., Gustafsson, K., Pettersson, B., & Colmsjö, A. (1997). Characterization of the cellulosic residues from lithium chloride/N,N-dimethylacetamide dissolution of softwood kraft pulp. *Carbohydrate Polymers*, *32*, 57–63.

Spence, K. L., Venditti, L. A., Rojas, O. J., Habibi, Y., & Pavlak, J. J. (2010). The effect of chemical composition on microfibrillar cellulose films from wood pulps: Water interaction and physical properties for packaging applications. *Cellulose*, *17*, 835–848.

Wickholm, K., Larsson, P. T., & Iversen, T. (1998). Assignment of non-crystalline forms in cellulose I by CP/MAS ^{13}C NMR spectroscopy. *Carbohydrate Research*, *312*, 123–129.